Electronic parameters and interfacial properties of GaAs/Al_xGa_{1-x}As multiquantum wells grown on (111)A GaAs by metalorganic vapor phase epitaxy

Soohaeng Cho, A. Sanz-Hervás,* and A. Majerfeld†
Department of Electrical and Computer Engineering, CB425, University of Colorado, Boulder, Colorado 80309, USA

B. W. Kim
Electronics and Telecommunications Research Institute, P.O. Box 106, Yusong, Taejon 305-600, Korea

(Received 18 October 2002; revised manuscript received 21 February 2003; published 10 July 2003)

We report a comprehensive study of the optical and interfacial properties of GaAs/Al_xGa_{1-x}As multiquantum wells grown on (111)A GaAs substrates by metalorganic vapor phase epitaxy which allowed the determination of the electronic parameters appropriate for such quantum wells. High-resolution x-ray diffractometry studies indicate an excellent crystal quality and good periodicity for the multiquantum wells and provided their structural parameters accurately. The photoreflectance spectra exhibit all the allowed and almost all the weakly allowed optical transitions between the confined hole and electron states. From an analysis of the photoreflectance spectra it is shown that the quantum well interfaces have an abruptness better than ± 1 ML. Photoluminescence spectroscopy was also performed to evaluate independently the roughness of the interfaces and multiquantum well period reproducibility. For a 25-period multiquantum well structure with a well width of 55 Å, a photoluminescence linewidth of 12.5 meV, which corresponds to a combined well-width fluctuation and interface roughness of less than ± 1 monolayer over the 25 periods, proves the achievement of heterointerfaces with excellent interfacial quality. From a detailed analysis of the high-order transitions observed in the photoreflectance spectra we determined key quantum well electronic parameters, such as, the heavy-hole valence-band offset $\boldsymbol{Q_v} = 0.33 \pm 0.02$, the transverse GaAs heavy-hole effective mass $m_{hh} = (0.95 \pm 0.02) m_0$, and the light-hole effective mass $m_{lh} = 0.08 m_0$ in $\langle 111 \rangle$ directions, for $\langle 111 \rangle$-oriented GaAs/Al_xGa_{1-x}As quantum well structures.

DOI: 10.1103/PhysRevB.68.035308 PACS number(s): 81.07.St, 78.67.De, 78.55.Cr, 61.10.Nz

I. INTRODUCTION

The growth of III–V compound semiconductors, such as GaAs and the related ternary alloys Al_xGa_{1-x}As and In_xGa_{1-x}As, in the nonconventional $\langle 111 \rangle$ crystallographic directions has attracted attention during the last few years due to their special physical and structural properties and their applicability to novel optoelectronic devices.[1,2] In particular, high quality GaAs/Al_xGa_{1-x}As quantum wells (QWs) are necessary for double confinement lasers. Surfaces normal to $\langle 111 \rangle$ orientations exhibit polar characteristics as they have either a Ga-terminated (111)A surface or an As-terminated (111)B surface. For this reason, epitaxial growth may evolve by the addition of discrete monolayers, which are composed of pairs of Ga and As layers, rather than by mixed atomic layers as for $\langle 100 \rangle$-oriented growth. This ordering of the atomic layers may improve the interface abruptness in heterostructures. Such naturally occurring flat interfaces between GaAs and Al_xGa_{1-x}As could enhance two-dimensional carrier mobility and the spectral quality of radiative transitions. It has been actually observed that structures grown on {111} substrates exhibit special or enhanced electrical and optical properties over those grown on conventional {100} substrates. For example, a significant reduction in the lasing threshold current density was achieved in GaAs/Al_xGa_{1-x}As lasers grown by molecular beam epitaxy (MBE) on slightly misoriented (111)B substrates.[3] Also, strained $\langle 111 \rangle$ layers exhibit the piezoelectric (PE) effect as well as the pyroelectric effect[4] and an enhanced quantum-confinement Stark shift due to the PE field. These effects can be exploited for novel device applications.[5] The $\langle 111 \rangle$ orientations may also allow the fabrication of high electron mobility transistors or lasers with extended characteristics.[6]

The status of the growth and the enhanced properties of bulk GaAs and Al_xGa_{1-x}As layers and GaAs/Al_xGa_{1-x}As QW structures grown on {111} GaAs substrates either by MBE or metalorganic vapor phase epitaxy (MOVPE) was summarized in a previous article.[7] We previously reported the successful growth of high quality GaAs/AlGaAs QW structures on (111)A GaAs substrates by MOVPE using a relatively low substrate temperature (600 °C).[7–9] In a recent letter[10] we presented a preliminary comparison of the interfacial properties of GaAs/Al_xGa_{1-x}As 25-period multi-QW (MQW) structures simultaneously grown on (111)A and (100) GaAs substrates by MOVPE. However, to the best of our knowledge, there has been no report on a comprehensive analysis of the interfacial properties of the (111)A GaAs/Al_xGa_{1-x}As material system. Furthermore, there is a considerable uncertainty about the appropriate values of the QW electronic parameters in $\langle 111 \rangle$ orientations, such as the transverse heavy-hole (m_{hh}) and light-hole (m_{lh}) effective masses for GaAs, as well as the heavy-hole valence-band offset, defined as $\boldsymbol{Q_v} = \Delta E_v / (\Delta E_c + \Delta E_v)$, where ΔE_c and ΔE_v are the conduction-band and heavy-hole valence-band offsets, respectively. Researchers employed different values of the heavy-hole valence-band offset $\boldsymbol{Q_v}$ for $\langle 111 \rangle$ GaAs/Al_xGa_{1-x}As structures, e.g., 0.32,[11] 0.33,[7–10] and 0.37.[3] However there has been no experimental study on a

 ©2003 The American Physical Society

systematic determination of $\boldsymbol{Q_v}$ for this material system in ⟨111⟩ directions. Similarly, although the effective masses for conventional ⟨100⟩ systems have been thoroughly studied, there is no consensus on the values of the effective masses for GaAs in ⟨111⟩ directions. Theoretically, a large anisotropy of the valence band is expected. There are only a few reports on the experimental determination of the transverse GaAs effective masses in ⟨111⟩ orientations. Hayakawa *et al.*[12] used the heavy-hole effective mass for GaAs as an adjustable parameter to fit the absorption spectra of (111)B GaAs/Al_xGa_{1-x}As MQW structures, obtaining $m_{hh}=0.90m_0$; these authors used a fixed value for the light-hole mass $m_{lh}=0.12m_0$. Kajikawa and co-workers[13,14] employed the same values and achieved consistent results in their study of the quantum-confinement Stark effect from a photocurrent spectroscopy study of *p-i-n* GaAs/Al_xGa_{1-x}As superlattice structures grown on (111)B GaAs substrates. Molenkamp *et al.*[11] interpreted the absorption spectra taking into account the effective mass anisotropy of the valence bands and they determined a heavy-hole effective mass $m_{\mathrm{hh}}=0.7m_0$; this value differs significantly from the value reported by Hayakawa *et al.*[12] It should be noted that in these studies[11–14] only a few transitions were considered, which may not be sufficient to allow a proper determination of the values for the effective masses. In addition, the structural quality of the samples used was not reported in detail. Recently, Los *et al.*[15] reported a theoretical calculation of the energy band structure and, thereby, the effective masses for QW structures for {111} and high-index surfaces.

The focus of the present work is on a detailed study of the optical, electronic and interfacial properties of (111)A GaAs/Al_xGa_{1-x}As MQW structures using various complementary techniques, such as HRXRD, low-temperature (LT, 11 K) photoreflectance (PR) spectroscopy, and LT PL spectroscopy. The HRXRD studies were performed to assess the crystallinity of the samples and to determine independently their structural parameters, which enabled us to analyze theoretically the optical measurements with fewer adjustable parameters. The PR measurements were conducted at LT to compare directly the lowest transition energy with the LT PL emission energy. The LT PR spectra exhibited all the allowed and almost all the weakly allowed transitions between confined electron and hole states in the QW. The experimental transition energies were determined by lineshape fitting of the PR spectra. We theoretically calculated the confined transition energies using the transfer matrix method assuming ideal square wells with varying width. In order to evaluate the abruptness of the MQW interfaces, we compared the experimental PR transition energies with the theoretically calculated energies for all the observed transitions, including the high-order transitions. In order to determine the QW electronic parameters, we also compared the experimental and theoretical transition energies using the QW electronic parameters as adjustable parameters. As a result, this analysis allowed us to determine quantitatively the QW electronic parameters for these MQW structures. In addition, the full-width-at-half-maximum (FWHM) of the LT PL emission between the lowest electron confined and lowest heavy-hole confined states was analyzed to provide an independent measure of the combined effect of well-width fluctuation (periodicity) and interface roughness. From the HRXRD studies, LT PR spectroscopy, LT PL spectroscopy, and the theoretical ML analysis we demonstrate the achievement of abrupt and smooth interfaces in GaAs/Al_xGa_{1-x}As MQW structures grown on (111)A GaAs substrates by MOVPE.

II. EXPERIMENTAL PROCEDURE

The samples studied in this work were grown in a horizontal quartz MOVPE reactor operated at atmospheric pressure.[7] We used undoped semi-insulating exactly oriented (111)A GaAs substrates. The substrates were degreased in organic solvents and were placed on a graphite susceptor during growth. We used 100% arsine, trimethylgallium, and trimethylaluminum as precursors. The carrier gas was *Pd*-diffused hydrogen with a total flow of 5 l/min. Before growth the substrates were baked for 7 min at 655 °C with arsine flow to remove native oxides from the surface. The growth temperature was 600 °C and the V/III molar ratios were 76 for the GaAs layers and 64 for the Al_xGa_{1-x}As layers, respectively. The GaAs/Al_xGa_{1-x}As QW structures analyzed have the following layer sequence in order of growth: (i) Sample MQ10: a 0.28-μm buffer, a ten-period GaAs/Al_xGa_{1-x}As MQW with an Al fraction of 29%, well and barrier lengths $L_w=105$ Å and $L_b=225$ Å, respectively, and a 46-Å GaAs cap on top (ii) Sample MQ25: a 0.38-μm buffer, a 25-period GaAs/Al_xGa_{1-x}As MQW with an Al fraction of 27%, well and barrier lengths $L_w=55$ Å and $L_b=235$ Å, respectively, and a 46-Å GaAs cap on top.

The HRXRD measurements were carried out with a Bede D^3 diffractometer. The x-ray beam was monochromatized ($\lambda=$Cu $K\alpha_1$) by using four consecutive (022) reflections on the 17.65°-off (011) surfaces of two Si channel-cut collimators. As the GaAs/Al_xGa_{1-x}As is a material system with very low lattice mismatch, no in-plane relaxation of the Al_xGa_{1-x}As layer is expected. Accordingly, we only measured $\theta/2\theta$ scans around the symmetric 333 reflection. The experimental diffraction profiles were fitted by computer-simulated diffraction curves based on the dynamical diffraction and anisotropic elasticity theories.[16]

Photoluminescence measurements at 11 K were performed using the 5145-Å line from an Ar^+ laser with an excitation intensity of 0.25 W/cm^2 and a double pass monochromator. Photoreflectance measurements at 11 K were made by using the beam from a tungsten light source passed through a double pass monochromator as the probe beam, with a chopped Ar^+ laser beam tuned to 5145 Å with an excitation intensity of 2.5 mW/cm^2 as the pump beam. A Si diode with a longpass filter (Corning 3-68) was used to detect the reflectance signal.

III. RESULTS AND DISCUSSION

In this section we present the experimental results obtained by different experimental techniques and a detailed analysis of the structural and physical properties of GaAs/Al_xGa_{1-x}As MQW grown on (111)A GaAs substrates by MOVPE.

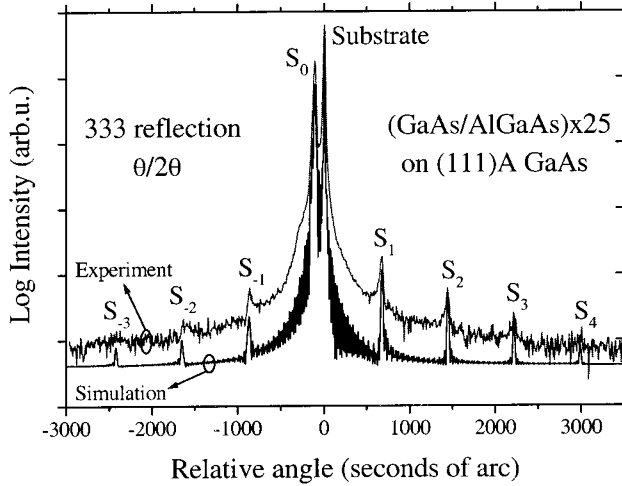

FIG. 1. HRXRD experimental profile and theoretical best-fit for the 25-period GaAs/Al_xGa_{1-x}As MQW grown on a (111)*A* GaAs substrate by MOVPE. The MQW satellites are marked by S_n, where *n* indicates the order.

A. High resolution x-ray diffractometry

Figure 1 shows the HRXRD experimental profile and the theoretical best-fit for sample MQ25. The experimental profile displays an intense narrow peak, originating from the substrate, and a set of MQW satellites S_n, where *n* indicates the order. The presence of distinct narrow satellites demonstrates that MQ25 has good crystal and interfacial qualities and periodicity. Theoretical dynamical computations were fitted to the experimental diffraction profile.[16] from which we accurately determined the MQW period length (L_P) and the average Al fraction in the period ($\langle x \rangle$). By taking into account the growth times of the GaAs and Al_xGa_{1-x} As layers,[17] we obtained unambiguously the Al fraction (x) of the Al_xGa_{1-x}As barriers and the quantum well (L_w) and barrier (L_b) lengths from the determined values of L_P and $\langle x \rangle$. For the calculation of x we used an Al_xGa_{1-x}As lattice parameter value resulting from the linear interpolation between the GaAs and AlAs values, which were taken as 5.6533 and 5.6622 Å respectively. The HRXRD profile for sample MQ10 indicated similarly good crystal quality, and periodicity. The structural values obtained from the HRXRD study of samples MQ25 and MQ10 are listed in Table I. The errors shown in Table I provide an estimation of the uncertainties associated with the fitting procedure. They do not represent variations of the structural values between different measurements, which are negligible for the present samples.

B. Low temperature photoreflectance spectroscopy

Low temperature PR spectroscopy was used to assess in detail the interfacial properties of the (111)*A* GaAs/Al_xGa_{1-x}As MQW structures and determine some of the QW electronic parameters. During a PR experiment the dielectric function, expressed by its real and imaginary parts $\varepsilon=\varepsilon_1+i\varepsilon_2$, is modulated by the chopped pump beam, producing a change in the measured reflectivity $\Delta R/R$ given by[18]

$$\frac{\Delta R}{R}=a(\varepsilon_1,\varepsilon_2)\Delta\varepsilon_1+b(\varepsilon_1,\varepsilon_2)\Delta\varepsilon_2, \tag{1}$$

where a and b are the Seraphin coefficients, and the quantities $\Delta\varepsilon_1$ and $\Delta\varepsilon_2$ are the changes of the real and imaginary parts of the dielectric function, respectively, induced by the modulating electric field created by the chopped pump beam. The modulated signal can be explained using a third-derivative of a Lorentzian function, which is expressed as[18,19]

$$\frac{\Delta R}{R}=\sum_{j=1}^{m}\left[A_j e^{i\phi_j}(E-E_j+i\Gamma_j)^{-n_j}\right], \tag{2}$$

where m is the total number of features in the spectrum, A_j is the amplitude, ϕ_j is a phase angle, E is the photon energy, E_j is the transition energy, and Γ_j is the broadening parameter of the jth feature. The exponent n_j is determined by the form of the dielectric function that is being modulated and by the modulation mechanism. In our case, the features in the PR spectra that were associated with the interband transitions were fitted using $n_j=3$, which corresponds to taking the third derivative of a two-dimensional critical point. The bulk GaAs and Al_xGa_{1-x}As features were fitted using $n_j=2.5$, which is the result of taking the third derivative of the three-dimensional critical points related to bulk GaAs and Al_xGa_{1-x}As. Besides the third-derivative of a Lorentzian function, there are two other types of lineshape functions that can be used to analyze PR spectra, namely, the first derivative of a Lorentzian function and the first derivative of a Gaussian function. However, it should be noted that the values of the QW confined transition energies extracted from such fits are generally insensitive to the choice of lineshape function.[20]

Figure 2 shows the 11-K PR spectra for (a) sample MQ25 and (b) sample MQ10. Shown by the solid lines in Fig. 2 are the least-squares fits of the experimental data to the relevant lineshape functions according to Eq. (2). The arrows in Fig.

TABLE I. Structural values obtained by HRXRD for the GaAs/Al_xGa_{1-x}As MQW structures grown on (111)*A* GaAs substrates by MOVPE. *N* is the number of periods, L_w, L_b, and L_{buffer} are the well, barrier, and buffer layer thickness, x is the Al fraction in the barriers, and r_{GaAs} and $r_{\mathrm{Al}_x\mathrm{Ga}_{1-x}\mathrm{As}}$ are the GaAs and Al_xGa_{1-x}As growth rates, respectively.

Sample	N	L_w (Å)	L_b (Å)	x	L_{buffer} (Å)	r_{GaAs} (Å/s)	$r_{\mathrm{Al}_x\mathrm{Ga}_{1-x}\mathrm{As}}$ (Å/s)
MQ10	10	105±5	225±5	28.8±1.0	2800±150	4.8±0.5	6.1±0.3
MQ25	25	55±5	237±5	26.5±1.0	3800±150	4.6±0.5	6.4±.0.3

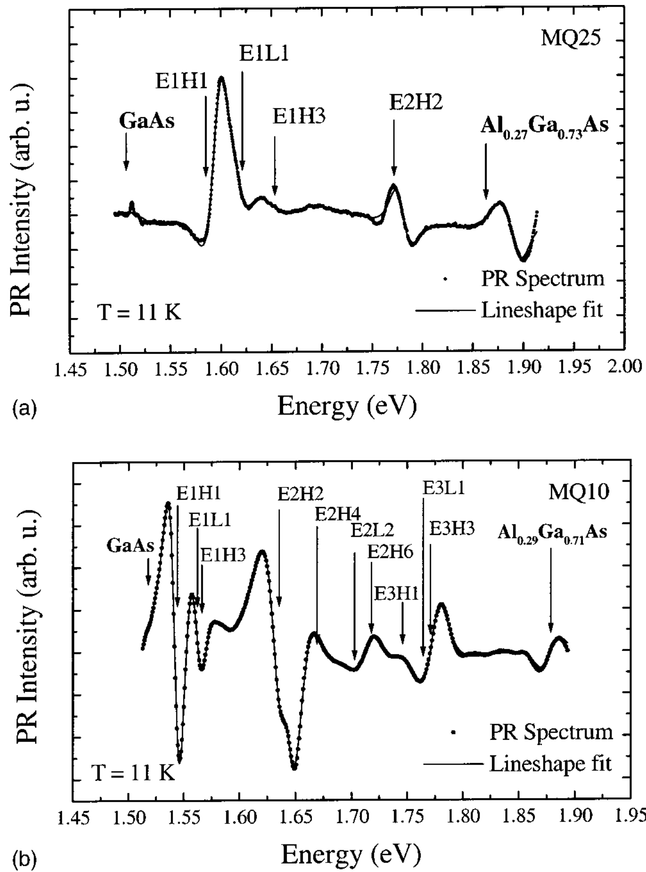

FIG. 2. PR spectra (dots) and theoretical best-fits (solid lines) for two GaAs/$Al_xGa_{1-x}As$ MQWs grown on (111)A GaAs substrates with (a) 25 periods and (b) ten periods.

2 indicate the values of the experimental transition energies deduced from the lineshape best-fit analyses. In order to identify the origin of the various spectral features observed in the PR spectra, we calculated the transition energies for the MQW structures within the transfer matrix formalism.[21] In the calculations an exciton binding energy of 6 meV was added to the measured values in order to determine the $Al_xGa_{1-x}As$ barrier bandgaps. The exciton binding energies for excitonic transitions were taken to be 8 meV for sample MQ10 (L_w = 105 Å), and 10 meV for sample MQ25 (L_w = 55 Å), respectively.[22] The effective masses that we tentatively used in the calculations were obtained by interpolating the theoretically determined Luttinger-Kohn parameters.[15] The heavy-hole valence-band offset $\boldsymbol{Q_v}$ was taken to be the conventional 33% of the total band-gap difference. The QW electronic parameters, such as, effective masses, bandgaps, and band offsets, for these two structures are listed in Table II. A detailed discussion about the adequacy of the values used for the effective masses and $\boldsymbol{Q_v}$ will be given in Sec. III C. The different transitions are labeled as EmH(L)n, which denotes a transition between the electron (E) mth conduction-band state and the nth valence-band state of heavy (H)- or light (L)-hole character.

According to our interpretation, for sample MQ25, we observed two electron conduction-band confined states, three heavy-hole and one light-hole valence-band confined states

TABLE II. Summary of the parameters used to calculate the transition energies for the GaAs/$Al_xGa_{1-x}As$ MQW structures grown on (111)A GaAs substrates. N is the number of periods, x is the Al fraction in the $Al_xGa_{1-x}As$ barriers, E_g is the band gap, m_e is the electron effective mass, m_{hh} is the heavy-hole effective mass, m_{lh} is the light-hole effective mass, ΔE_c is the conduction-band offset, and ΔE_v is the valence-band offset.

Parameter	Sample MQ10	Sample MQ25
N	10	25
x (%)	29	27
E_g of $Al_xGa_{1-x}As$ (eV)	1.884[a]	1.868[a]
$m_e/m_0(Al_xGa_{1-x}As)$	0.087	0.084
$m_{hh}/m_0(Al_xGa_{1-x}As)$	1.002	0.999
$m_{lh}/m_0(Al_xGa_{1-x}As)$	0.093	0.092
$m_e/m_0(GaAs)$	0.067	0.067
$m_{hh}/m_0(GaAs)$	0.952	0.952
$m_{lh}/m_0(GaAs)$	0.079	0.079
ΔE_c (meV)	245	234
ΔE_v (meV)	120	115

[a]After adding an exciton binding energy of 6 meV.

inside the wells. The experimental energies were completely identified with all the allowed transitions (E1H1, E1L1, and E2H2) and one weakly allowed transition (E1H3) for this structure along with the $Al_xGa_{1-x}As$-related peak at 1.862 eV.

We applied the same method to analyze the PR spectrum of sample MQ10. This sample has wider wells (L_w = 105 Å) than MQ25 (L_w = 55 Å) and, therefore, has more confined interband transitions for a similar Al fraction. The larger number of transitions allowed us to obtain a better accuracy both in the assessment of the interface abruptness and in the determination of the QW electronic parameters, as will be described in Sec. III C. For sample MQ10, from the line-shape fitting it was possible to identify five allowed transitions (E1H1, E1L1, E2H2, E2L2, and E3H3) and five weakly allowed transitions (E1H3, E2H4, E2H6, E3H1, and E3L1) between the three electron states in the conduction-band and six heavy-hole and two light-hole states in the valence band. The weakly allowed E1H5 and E3H5 transitions were not observed. This can be attributed to the fact that the amplitudes of those transitions are small compared to the other transitions. There is an additional peak at 1.878 eV, which is related to the $Al_xGa_{1-x}As$ barriers.

A comparison between the experimental transition energies obtained from the PR spectra and the theoretically calculated transition energies taking into account the exciton binding energies[22] is summarized in Table III. The excellent agreement between the experimental and calculated transition energies, to within a few millielectronvolts, reveals a high degree of structural quality and uniformity of the interfaces, which is essential for obtaining appropriate QW electronic parameters by the method which will be discussed in Sec. III C. The PR features related to the $Al_xGa_{1-x}As$ barriers enabled us to measure directly the band gap (E_g) and the Al fraction (x) of the $Al_xGa_{1-x}As$ barriers. The dependence of the $Al_xGa_{1-x}As$ band gap with the Al fraction x at 11 K is

TABLE III. Comparison between the experimental transition energies deduced from the best line-shape fit to 11-K PR spectra and the theoretical calculations for the ten- and 25-period GaAs/$Al_xGa_{1-x}As$ MQWs grown on (111)*A* GaAs substrates.

Ten-period MQW (sample MQ10) $L_w = 105$ Å			25-period MQW (sample MQ25) $L_w = 55$ Å		
Spectral feature	PR energy (eV)	Calculation[a] (eV)	Spectral feature	PR energy (eV)	Calculation[a] (eV)
$Al_{0.29}Ga_{0.71}As$	1.878	-	$Al_{0.27}Ga_{0.73}As$	1.863	-
E1H1	1.543	1.543	E1H1	1.586	1.586
E1L1	1.561	1.561	E1L1	1.622	1.623
E1H3	1.565	1.565	E1H3	1.653	1.652
E1H5	not observed	1.610	E2H2	1.771	1.770
E2H2	1.635	1.635			
E2H4	1.669	1.669			
E2L2	1.703	1.704			
E2H6	1.722	1.722			
E3H1	1.745	1.745			
E3L1	1.764	1.764			
E3H3	1.771	1.768			
E3H5	not observed	1.813			

[a]After deducing an exciton binding energy of 8 meV for the ten-period MQW and 10 meV for the 25-period MQW (Ref. 20).

given by $E_g(\mathrm{eV}) = 1.519 + 1.247x (x < 40\%)$.[23] For sample MQ10, the 1.878 eV feature gives $x = 29\%$ and for sample MQ25 the 1.862-eV feature yields $x = 27\%$. These two values are in excellent agreement with the Al fractions obtained from the independent HRXRD analysis (shown in Table I).

C. Quantitative determination of ⟨111⟩ QW electronic parameters: Heavy-hole valence-band offset and transverse GaAs heavy and light-hole effective masses

As summarized in Sec. I, due to the relative novelty of the epitaxial growth of the GaAs/$Al_xGa_{1-x}As$ materials system on {111} surfaces compared to the (100) case, fundamental QW electronic parameters, such as, the heavy-hole valence-band offset $\boldsymbol{Q_v}$, and the effective masses, are not presently well established. For this reason, the principal objective of this work was the experimental determination of $\boldsymbol{Q_v}$ and the transverse GaAs heavy-hole and light-hole effective masses for ⟨111⟩-oriented GaAs/$Al_xGa_{1-x}As$ QWs. For this reason the structural parameters of the MQW and a detailed knowledge of the heterointerfaces are of key importance. In order to ascertain the best value of $\boldsymbol{Q_v}$ for our MQW structures, we compared the theoretically calculated transition energies with the experimental PR transition energies using $\boldsymbol{Q_v}$ as the only adjustable parameter in the calculations. The calculated transition energies as a function of $\boldsymbol{Q_v}$ are shown in Fig. 3 for both samples (MQ10, MQ25). The tentative values of the effective masses used in the calculations are listed in Table II. These theoretical values were obtained from Ref. 15 and their appropriateness will be discussed later. In Fig. 3 the solid lines represent the calculated values for the transition energies and the horizontal dashed lines show the experimental energies obtained by fitting the PR spectra. The vertical dotted lines represent the value of $\boldsymbol{Q_v}$ that provides the best agreement for both MQ10 and MQ25 samples. A detailed discussion of these results is summarized in the following comments.

(i) The choice of $\boldsymbol{Q_v}$ as an adjustable parameter in the calculations is justified by the fact that the high-order transitions, which are located near the top of the wells, are strongly dependent on the energy depth of the wells, and thus

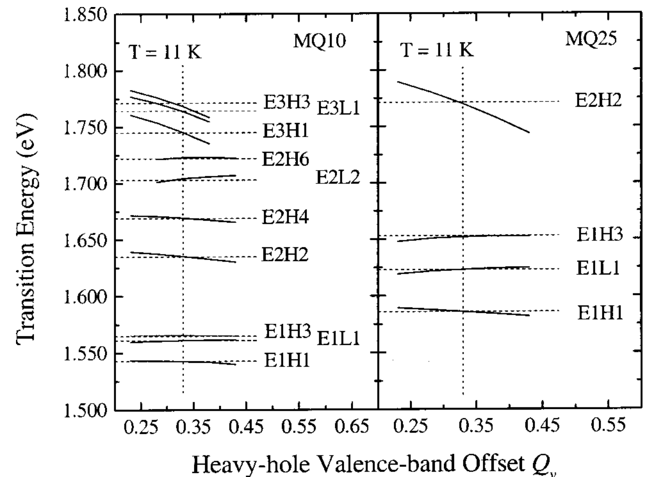

FIG. 3. Calculated transition energies as a function of the heavy-hole valence-band offset $\boldsymbol{Q_v}$ for the ten-period (MQ10, left) and 25-period (MQ25, right) GaAs/$Al_xGa_{1-x}As$ MQWs grown on (111)*A* GaAs substrates. The solid lines are the calculated transition energies for varying $\boldsymbol{Q_v}$ and the dashed horizontal lines indicate the experimental energies obtained by fitting the PR spectra. The vertical dotted lines show the value of $\boldsymbol{Q_v}$ that gives the best fit to all the observed PR transitions.

on Q_v. It must be noted that the energy band gap of the $Al_xGa_{1-x}As$ barrier layers was directly measured by LT PR. Furthermore, the PR feature yields an Al fraction which is in excellent agreement with the HRXRD studies. Therefore, there is no uncertainty about the bandgap value in our samples, and Q_v remains as the only parameter that can significantly affect the potential energy depth of the well.

(ii) For sample MQ10, some of the observed transitions in the experimental PR spectrum cannot be obtained from the theoretical calculations using heavy-hole valence-band offset Q_v values lower than 0.28 or higher than 0.38. This is so because the number of confined states in the conduction- or valence-band is critically dependent on the barrier height and, therefore, on the valence-band offset. This observation alone limits the range ($0.28 < Q_v < 0.38$) of possible Q_v values for sample MQ10. Furthermore, for the MQ25 sample, the highest confined states, both in the conduction (E2) and valence band (H3), emerge in the calculations using the range of Q_v values mentioned above.

(iii) By comparing the experimental results to our calculated values, it is concluded that the best value for Q_v is 0.33 ± 0.02. The error represents one standard deviation of the values obtained for all the observed transitions. This value obtained for $\langle 111 \rangle$-oriented $GaAs/Al_xGa_{1-x}As$ QWs is similar to the value for $\langle 100 \rangle$ QWs.

(iv) It is important to note that all the calculated transition energies do not change in the same direction when the band offset is increased. This indicates that, even though the transition energies are also a function of the effective mass, a change of the effective mass does not reverse the trend of any particular transition energy to increase or decrease with band offset changes. Therefore, it is not possible to achieve such a good agreement between all the experimental and calculated transition energies only by changing the effective mass and using a value of Q_v other than 0.33.

(v) The fact that the calculated transition energies agree well with the observed transitions assures that the obtained Q_v is a reliable determination.

From the above analysis we determined the best value of the heavy-hole valence-band offset Q_v for our (111)A $GaAs/Al_xGa_{1-x}As$ MQW structures by tentatively accepting certain theoretical values for the effective masses as listed in Table II. In what follows we discuss the experimental determination of the transverse GaAs effective masses.

From the band energy dispersion relation, the heavy-hole and the light-hole effective masses along the $\langle 111 \rangle$ growth directions are given by

$$m_{hh}^{(111)} = \frac{m_0}{\gamma_1 - 2\gamma_3}, \tag{3a}$$

$$m_{lh}^{(111)} = \frac{m_0}{\gamma_1 + 2\gamma_3}, \tag{3b}$$

where γ_1 and γ_3 are the Luttinger-Kohn parameters. The theoretical heavy-hole and light-hole effective masses for GaAs and $Al_xGa_{1-x}As$ layers are calculated using Eqs. (3a) and (3b) by linearly interpolating the theoretical Luttinger-Kohn parameters for GaAs ($\gamma_1 = 6.85, \gamma_3 = 2.9$) and AlAs ($\gamma_1 = 3.45, \gamma_3 = 1.29$).[15] The electron effective masses for $Al_xGa_{1-x}As$ layers are also obtained by linear interpolation between the GaAs ($0.067m_0$) and AlAs ($0.124m_0$) values.[15] The theoretical transverse effective mass values for our samples MQ10 and MQ25 are listed in Table II. To establish the best value of the GaAs effective masses for our samples, we calculated the dependence of the transition energies on the heavy-hole effective mass. For the valence-band offset Q_v we used the previously determined value of 0.33. The result of those computations is shown in Fig. 4, in which only the heavy-hole related transitions are displayed. The solid lines represent the calculated transition energies and the horizontal dashed lines indicate the PR experimental transition energies. It can be seen that the high-order transitions are more sensitive to the variation of the effective mass than the low-order transitions. The dashed vertical lines mark the best value $m_{hh} = (0.95 \pm 0.02)m_0$ for the transverse GaAs heavy-hole effective mass for both samples, which is in agreement with the theoretical value.[15] The error represents one standard deviation of the values obtained for all the observed transitions. Regarding the light-hole mass, as the PR spectra exhibited only a few light-hole related transitions, it was not possible to employ this fitting procedure with enough accuracy, therefore, we used the theoretical value of $m_{lh} = 0.08m_0$ obtained from Eq. (3b), which is significantly different from the value previously reported.[12–14] In view of the good agreement that was achieved for all the observed transitions using this theoretical value, we conclude that both the heavy-hole and light-hole effective masses used in the calculations are at the very least consistent with the experimental results. It should be noted that our value for the transverse GaAs heavy-hole effective mass ($m_{hh} = 0.95m_0$) is much larger than that for the [100] orientation ($0.34m_0$).

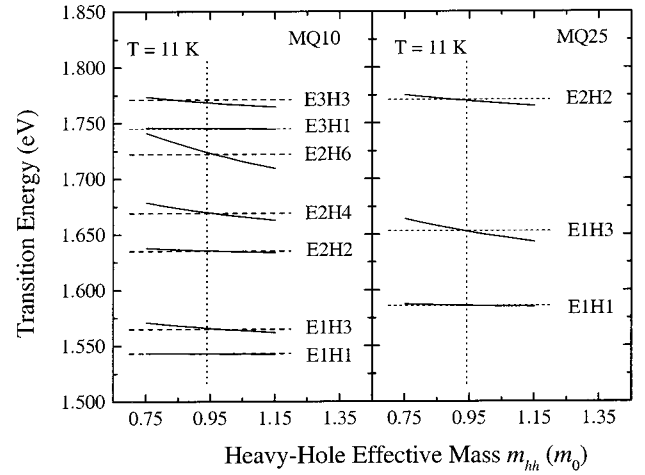

FIG. 4. Calculated heavy-hole related transition energies as a function of the transverse GaAs heavy-hole effective mass (m_{hh}) for the ten, (MQ10, left) and 25-period (MQ25, right) $GaAs/Al_xGa_{1-x}As$ MQWs grown on (111)A GaAs substrates. A heavy-hole valence-band offset $Q_v = 0.33$ was used. The solid lines are the calculated transition energies for varying m_{hh} and the dashed horizontal lines indicate the experimental energies obtained by fitting the PR spectra. The vertical dotted lines show the value of m_{hh} that provides the best fit to all the transitions.

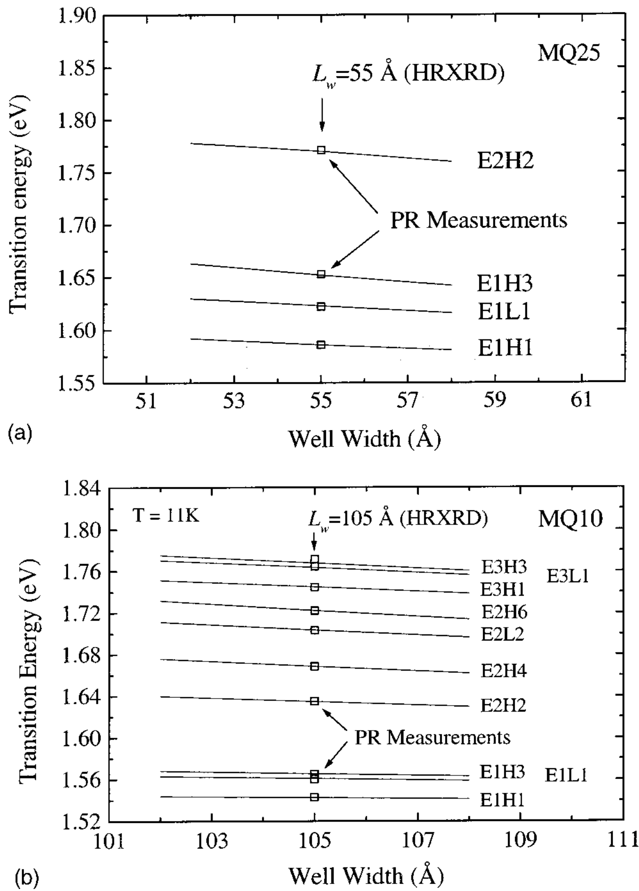

FIG. 5. Variation of the theoretical transition energies (solid lines) as a function of well width for the GaAs/$Al_xGa_{1-x}As$ MQWs grown on (111)A GaAs substrates with (a) 25 periods and (b) ten periods. The hollow squares show the observed experimental PR transition energies.

Therefore, we obtained a larger effective-mass anisotropy than in previous reports. While in our case the ratio $m_{hh}(111)/m_{hh}(100)$ equals 2.80, this ratio is 2.06 for Molenkamp *et al.*,[11] 2.53 for Hess *et al.*[25] 2.60 for Lawaetz *et al.*,[24] and 2.65 for Hayakawa *et al.*[3] It must be noted at this point that, as the experimental value for the heavy-hole effective mass is in perfect agreement with the tentative theoretical value used previously in the evaluation of the heavy-hole valence-band offset Q_v, the value obtained for Q_v is still valid and does not have to be reevaluated. In summary, we achieved a consistent explanation of the observed PR transition energies using the values $Q_v = 0.33 \pm 0.02$, $m_{hh} = (0.95 \pm 0.02) m_0$, and $m_{lh} = 0.08 m_0$ for ⟨111⟩-oriented GaAs/$Al_xGa_{1-x}As$ QW structures.

D. Evaluation of interface abruptness: ML analysis

In order to evaluate the abruptness and uniformity of the interfaces of the MQW structures, we carried out a ML analysis, which involves a comparison between the experimental transition energies obtained from the PR spectra and the theoretical transition energies calculated for a varying well width. Figure 5 shows the calculated transition energies for different well widths in the range $L_w \pm 1$ ML [1 ML $= \sqrt{3} a_L / 3 = 3.26$ Å in ⟨111⟩ GaAs, where a_L is the lattice constant of GaAs] for (a) sample MQ25 and (b) sample MQ10 under the assumption that the QWs are perfectly square. The solid lines indicate calculated transition energies, which are a function of the well width, and the hollow squares show the experimental PR transition energies. The QW transition energies are dependent on the well width. It can be seen that all the experimental transition energies are well within the range of the calculated values for a well width $L_w \pm 1$ ML, where the L_w was obtained from the HRXRD study. If the actual potential profile in the MQW structure was non-square, the transition energies, especially for the high-order transitions, should significantly shift, which would not allow to achieve such a good agreement between the experimental and the theoretical transition energies for all the observed transitions, particularly for the high-order transitions. Therefore, the excellent agreement (to within 3 meV) between all the experimental and theoretical transition energies, as shown in Fig. 5 and Table III indicates that our samples have an interface abruptness better than ± 1 ML. This result provides further confirmation that the wells of the MQW structures investigated are essentially square.

E. Evaluation of interface roughness and well-width fluctuation: PL analysis

In a periodic MQW structure, the broadening of the FWHM of the PL emission peak is mainly due to the combined effects of well-width fluctuation from well to well in the periodic structure and interface roughness. Accordingly, the PL FWHM was analyzed to assess the interfacial properties of the (111)A GaAs/$Al_xGa_{1-x}As$ MQW structures. Figure 6 shows the PL spectrum at 11 K for sample MQ25. The PL analysis of sample MQ10 was reported elsewhere.[8] The MQ25 LT PL peak energy ($E_p = 1.585$ eV) corresponds to the radiative transition between the confined states E1 and H1 and, as expected, is in perfect agreement with the value observed in the LT PR spectrum (see Table III). The FWHM of 12.5 meV is smaller than the energy difference for the E1H1 transition calculated for the well widths $L_w - 1$ ML and $L_w + 1$ ML, as can be seen in Fig. 5(a). Therefore, it is concluded that the combined well-width fluctuation and interface roughness of sample MQ25 must be less than ± 1 ML over the 25 periods of the MQW structure. This result indicates that the sample has excellent interfacial quality and period repeatability. Previously, Chin *et al.* reported a FWHM of 13.4 meV for a five-period MQW grown on a (111)A GaAs substrate by MBE with a well width of 100 Å.[26] Sanz-Hervás *et al.*[10] reported a FWHM of 10.5 meV for a similar structure (25-period GaAs/$Al_xGa_{1-x}As$ MQW) with a narrower well width ($L_w = 44$ Å). A FWHM of 12.5 meV for sample MQ25 is therefore among the best values reported for GaAs/$Al_xGa_{1-x}As$ MQWs grown on (111)A GaAs substrates either by MBE or MOVPE. Several authors have recently reported that, even in highly lattice-mismatched materials systems, such as, InAs/GaAs (Refs. 27 and 28) or InSb/GaAs.[29] (111)A GaAs substrates appear to provide naturally atomically flat interfaces for MBE growth. In the present study we have shown the achievement of very

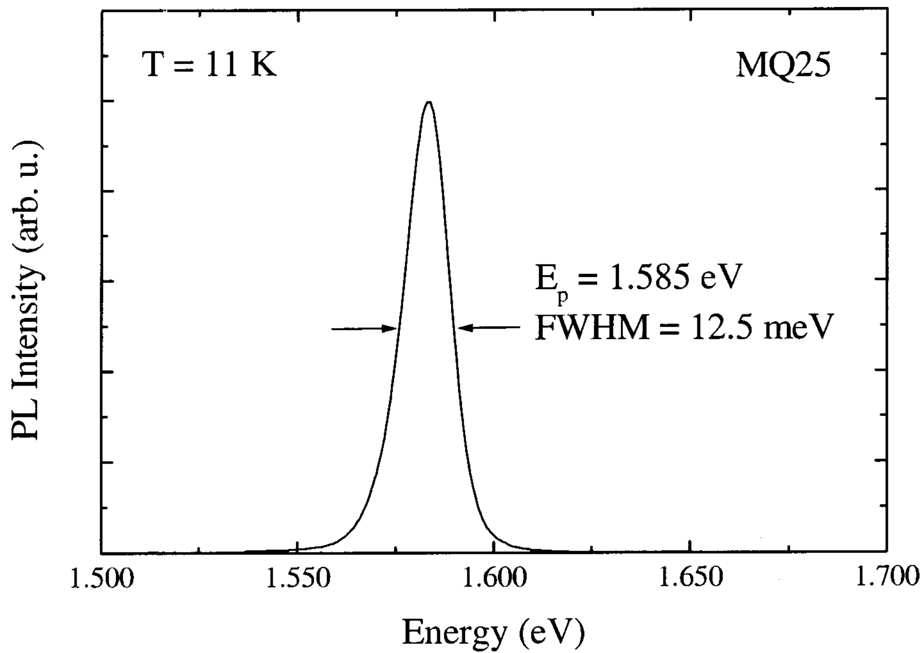

FIG. 6. PL spectrum for the 25-period $GaAs/Al_xGa_{1-x}As$ MQW grown on a (111)A GaAs substrate. E_p is the PL peak energy.

abrupt and uniform interfaces in $GaAs/Al_xGa_{1-x}As$ QW structures grown by MOVPE on (111)A GaAs. Very recent results[9,30] indicate that similar interfacial quality can be achieved in strained $In_xGa_{1-x}As$/GaAs QW structures grown on GaAs (111)A substrates by MOVPE. Thus, it can be concluded that QWs with good interfacial properties can be obtained on the (111)A surface regardless of the epitaxial growth technique employed.

IV. SUMMARY AND CONCLUSIONS

In summary, we reported the determination of the electronic parameters and the optical and interfacial properties of $GaAs/Al_xGa_{1-x}As$ MQW structures grown on (111)A GaAs substrates by MOVPE. The HRXRD study shows the excellent crystal quality and very good QW periodicity of the samples. The PR spectra exhibit all the_allowed and almost all the weakly allowed optical transitions. The experimental transition energies are in excellent agreement with the theoretically calculated values, from which we showed that the QW interfaces have an abruptness better than ±1 ML. For the 25-period MQW a PL FWHM of 12.5 meV was observed, which corresponds to a combined interface roughness and well-width (55 Å) fluctuation over the 25 periods of less than ±1 ML, and proves the excellent interfacial quality and period repeatability in this structure. The PL FWHM value of 12.5 meV for the 25-period MQW is among the narrowest values reported for (111)A MQWs grown by MOVPE or MBE. These results indicate the achievement of 1–2-ML heterointerfaces for (111)A $GaAs/Al_xGa_{1-x}As$ QW structures grown by MOVPE. The high quality of these QW structures allowed us to determine accurately the values of the heavy-hole valence-band offset $\boldsymbol{Q_v}$ and the transverse GaAs heavy-hole and light-hole effective masses, which were not well established for the ⟨111⟩ crystallographic orientations, by comparing the experimental PR transitions with the theoretical transition energies computed for a range of values for each QW electronic parameter. For (111)A $GaAs/Al_xGa_{1-x}As$ MQWs we obtained a heavy-hole valence-band offset $\boldsymbol{Q_v}=0.33\pm0.02$ and the transverse GaAs heavy-hole and light-hole effective masses in the ⟨111⟩ directions; $m_{hh}=(0.95\pm0.02)m_0$ and $m_{lh}=0.08m_0$, respectively. The effective masses are significantly different from the values previously reported but in excellent agreement with the theoretically expected values. Finally, the achievement of abrupt and smooth QW interfaces on the (111)A surface by MOVPE indicates the feasibility of fabricating QW devices employing the special properties of the ⟨111⟩ orientations.

ACKNOWLEDGMENTS

The work at the University of Colorado was supported by the Electronics and Telecommunications Research Institute (Taejon, Korea). One of us (A.S.-H.) wishes to acknowledge partial financial support by U.P.M. (Madrid, Spain). We wish to thank C. Villar for some of the HRXRD measurements and R. Melliti, G. Wang, and P. Tronc (E.S.P.C.I., Paris, France) for very valuable discussions.

*On leave from Dpto. de Tecnología Electrónica, E.T.S.I. Telecomunicación, Universidad Politécnica de Madrid, Ciudad Universitaria, 28040 Madrid, Spain.

†Author to whom correspondence should be addressed. E-mail address: majerfel@spot.colorado.edu

[1] C. Mailhiot and D. L. Smith, Phys. Rev. B **35**, 1242 (1987).

[2] J. L. Sánchez-Rojas, A. Sacedón, E. Calleja, E. Muñoz, A. Sanz-Hervás, G. de Benito, and M. López, Phys. Rev. B **53**, 15 469 (1996).

[3] T. Hayakawa, T. Suyama, K. Takahashi, M. Kondo, S. Yamamoto,

and T. Hijikata, Appl. Phys. Lett. **52**, 339 (1988).

[4] Soohaeng Cho, A. Majerfeld, A. Sanz-Hervás, J. J. Sánchez, J. L. Sánchez-Rojas, and I. Izpura, J. Appl. Phys. **90**, 915 (2001).

[5] K. W. Goossen, E. A. Caridi, T. Y. Chang, J. B. Stark, D. A. B. Miller, and R. A. Morgan, Appl. Phys. Lett. **56**, 715 (1990).

[6] T. Fleischmann, M. Moran, M. Hopkinson, H. Meidia, G. J. Rees, A. G. Cullis, J. L. Sánchez-Rojas, and I. Izpura, J. Appl. Phys. **89**, 4689 (2001).

[7] A. Sanz-Hervás, Soohaeng Cho, Jongseok Kim, A. Majerfeld, C. Villar, and B. W. Kim, J. Cryst. Growth **195**, 558 (1998).

[8] A. Sanz-Hervás, Soohaeng Cho, O. V. Kovalenkov, S. A. Dickey, A. Majerfeld, C. Villar, M. López, R. Melliti, G. Wang, P. Tronc, and B. W. Kim, Inst. Phys. Conf. Ser. No. 156 (IEEE, New York, 1998), p. 291.

[9] Soohaeng Cho, A. Sanz-Hervás, Jongseok Kim, A. Majerfeld, C. Villar, and B. W. Kim, Microelectron. J. **30**, 455 (1999).

[10] A. Sanz-Hervás, Soohaeng Cho, A. Majerfeld, and B. W. Kim, Appl. Phys. Lett. **76**, 3073 (2000).

[11] L. W. Molenkamp, R. Eppenga, G. W. ’t Hooft, P. Dawson, C. T. Foxon, and K. J. Moore, Phys. Rev. B **38**, 4314 (1988).

[12] T. Hayakawa, K. Takahashi, M. Kondo, T. Suyama, S. Yamamoto, and T. Hijikata, Phys. Rev. Lett. **60**, 349 (1988).

[13] Y. Kajikawa, N. Sugiyama, T. Kamijoh, and Y. Katayama, Jpn. J. Appl. Phys. **28**, L1022 (1989).

[14] Y. Kajikawa, M. Hata, N. Sugiyama, and Y. Katayama, Phys. Rev. B **42**, 9540 (1990).

[15] J. Los, A. Fasolino, and A. Catellani, Phys. Rev. B **53**, 4630 (1996).

[16] A. Sanz-Hervás, M. Aguilar, J. L. Sánchez-Rojas, A. Sacedón, E. Calleja, E. Muñoz, C. Villar, E. J. Abril, and M. López, J. Appl. Phys. **82**, 3297 (1997).

[17] Y. Finkelstein, E. Zolotoyabko, M. Blumina, and D. Fekete, J. Appl. Phys. **79**, 1869 (1996).

[18] D. E. Aspnes, *Handbook on Semiconductors* (North-Holland, New York, 1980), Vol. 2, p. 109.

[19] O. J. Glembocki and B. V. Shanabrook, Superlattices Microstruct. **3**, 235 (1987).

[20] Y. S. Huang, H. Qiang, F. H. Pollak, J. Lee, and B. Elman, J. Appl. Phys. **70**, 3808 (1991).

[21] B. Jonsson and T. E. Eng, IEEE J. Quantum Electron. **26**, 2025 (1990).

[22] L. Viña, L. Muñoz, F. Calle, N. Mestres, J. M. Calleja, and W. I. Wang, Phys. Rev. B **46**, 13 234 (1992).

[23] H. C. Casey, and M. B. Panish, *Heterostructure Lasers* (Academic Press, New York, 1978), Pt. A, p. 187.

[24] P. Lawaetz, Phys. Rev. B **4**, 3460 (1971).

[25] K. Hess, D. Bimberg, N. O. Lipari, J. U. Fischbach, and M. Altarelli, in *Proceedings of the Thirteenth International Conference on the Physics of Semiconductors* (North-Holland, Amsterdam, 1976), p. 142.

[26] A. Chin and K. Lee, Appl. Phys. Lett. **68**, 3437 (1996).

[27] H. Yamaguchi, M. R. Fahy, and B. A. Joyce, Appl. Phys. Lett. **69**, 776 (1996).

[28] B. A. Joyce, T. S. Jones, and J. G. Belk, J. Vac. Sci. Technol. B **16**, 2373 (1998).

[29] K. Kanisawa, H. Yamaguchi, and Y. Hirayama, Appl. Phys. Lett. **76**, 589 (2000).

[30] Jongseok Kim, Soohaeng Cho, A. Sanz-Hervás, A. Majerfeld, and B. W. Kim, J. Cryst. Growth **225**, 415 (2001).